Received: 1 February 2021 | Revised: 24 February 2021 | Accepted: 4 March 2021

DOI: 10.1002/jhet.4257

ARTICLE

JOURNAL OF HETEROCYCLIC CHEMISTRY WILEY

Synthesis of antimicrobial azoloazines and molecular docking for inhibiting COVID-19

Zeinab A. Muhammad[1] | **Thoraya A. Farghaly**[2,3] | **Ismail Althagafi**[3] | **Sami A. Al-Hussain**[4] | **Magdi E. A. Zaki**[4] | **Marwa F. Harras**[5]

[1]Department of Organic Chemistry, National Organization for Drug Control and Research (NODCAR), Giza, Egypt

[2]Department of Chemistry, Faculty of Science, Cairo University, Giza, Egypt

[3]Department of Chemistry, Faculty of Applied Science, Umm Al-Qura University, Makkah, Saudi Arabia

[4]Department of Chemistry, Faculty of Science, Al-Imam Mohammad Ibn Saud Islamic University (IMSIU), Riyadh, Saudi Arabia

[5]Department of Pharmaceutical Chemistry, Faculty of Pharmacy (Girls), Al-Azhar University, Cairo, Egypt

Correspondence
Thoraya A. Farghaly, Department of Chemistry, Faculty of Science, Cairo University, Giza, 12613, Egypt.
Email: thoraya-f@hotmail.com; tamohamed@uqu.edu.sa

Diverse new azoloazines were synthesized from the reaction of fluorinated hydrazonoyl chlorides with heterocyclic thiones, 1,8-diaminonaphthalene, ketene aminal derivatives, and 4-amino-5-triflouromethyl-1,2,4-triazole-2-thiol. The mechanistic pathways and the structures of all synthesized derivatives were discussed and assured based on the available spectral data. The synthesized azoloazine derivatives were evaluated for their antifungal and antibacterial activities through zone of inhibition measurement. The results revealed promising antifungal activities for compounds **4**, **5**, **17a**,**b**, **19**, and **25** against the pathogenic fungal strains used; *Aspergillus flavus* and *Candida albicans* compared to ketoconazole. In addition, compounds **4**, **5**, **19**, and **25** showed moderate antibacterial activities against most tested bacterial strains. Molecular docking studies of the promising compounds were carried out on leucyl-tRNA synthetase active site of *Candida albicans*, suggesting good binding in the active site forming stable complexes. Moreover, docking of the synthesized compounds was performed on the active site of SARS-CoV-2 3CLpro to predict their potential as a hopeful anti-COVID and to investigate their binding pattern.

1 | INTRODUCTION

Multidrug resistance of several strains of microorganisms, due to antibiotics misuse, has been emerged as one of the main serious problems.[1] Thus, novel antimicrobial drugs with new targets should be developed to overcome the increased occurrence of microbial resistance. Additionally, the increased incidences of fungal infections in an invasive form, particularly in immune-compromised patients, have led to many deaths globally.[2] Accordingly, the need for novel antifungal agents is also an increasing concern. The leucyl-tRNA synthetase is one of the highly validated targets for antimicrobial agents. It plays a key role in the tRNA aminoacylation and synthesis of the microbial proteins. The effective antifungal, 5-fluoro-1,3- dihydro-1-hydroxy-2,1-benzoxaborole (AN2690), was reported to inhibit leucyl-tRNA synthetase by trapping the editing site of the enzyme.[3–5] From another side, triazolopyrimidines showed in several reports different types of potent biological activities including antimalarial,[6] anti-Alzheimer,[7] antihypertensive,[8] leishmanicidal cardiac stimulant,[9] anti-HBV,[10] antifungal,[11] anticancer,[12] antimicrobial,[11] and herbicidal activities.[13] Pogaku and coworkers synthesized new derivatives of triazolopyrimidine, which revealed α-glucosidase inhibitor activity.[14] In addition, the presence of fluoride atom on the skeleton of heterocyclic drugs improves their activity.[15,16]

Recently, the widespread of COVID-19, caused by the new coronavirus 2 (SARS-CoV-2), all over the world has emerged as a serious concern to public health.[17] Up to now, millions of infections and deaths have been recorded worldwide. In this consequence, there is a critical need for new antiviral agents targeting the virus life

cycle, membrane fusion, or the virus replication.[18] The main protease affords a greatly validated antiviral target for the design and discovery of inhibitors. SARS-CoV-2 main protease (Mpro) is a vital protein in the lifecycle of SARS-CoV, making it an ideal target to anti-COVID-19 agents.[19–21] All previous facts, together with our experiences in the field of synthesizing bioactive heterocyclic ring systems,[22–32] lead us in this context to synthesize new fluorinated derivatives of triazolopyrimidines pyridopyrimidine, naphthodiazipene, triazolothiadiazine, and triazolotetrazine. The newly synthesized azoloazine derivatives were evaluated for their antimicrobial activities against different antibacterial and antifungal strains. Moreover, molecular docking analysis was done to predict the possible binding interactions between derivatives with promising activities and the editing domain of leucyl-tRNA synthetase. Furthermore, a docking study of the synthesized compounds was used to demonstrate the probability of these compounds to inhibit SARS-CoV-2 main protease.

2 | RESULTS AND DISCUSSION

Several reviews and our previous articles[33–37] indicated the efficacy of the various derivatives of hydrazonoyl halides in the synthesis of bioactive heterocyclic systems. Herein, we used two fluorinated hydrazonoyl chlorides **4** and **5** to synthesis fused azole derivatives. Scheme 1 indicates the synthetic procedure of the two reactive fluorinated hydrazonoyl chlorides as described previously in our lab.[38]

Firstly, the two hydrazonoyl chlorides **4** and **5** were reacted with quinazoline-2-thione derivative **6** in dioxane/Et_3N as indicated in the experimental part to afford [1,2,4]triazolo[3,4-*b*]quinazoline derivatives **9a**,**b**. The structure of the latter products **9a**,**b** were assured based on the data obtained from their spectral data and their comparison with the literature reports. The disappearance of the absorption band for the carbonyl group from the IR spectra of the products **9a**,**b** proved the cyclized products of such reactions. Moreover, ^{1}H NMR of the two derivatives **9a**,**b** were free from any NH signals and showed the expected aliphatic and aromatic protons' signals. The suggested pathway for the formation of [1,2,4]triazolo[3,4-*b*]quinazoline derivatives **9a**,**b** is outlined in Scheme 2, starting from the formation substituted intermediate **7** followed by the smiles rearrangement[39] to give the intermediate **8**. Cyclization of the intermediate **8** with elimination of H_2S molecule afforded the target products **9a**,**b**.

Target triazolopyrimidines **13a-d** have been synthesized through the same pathway as compounds **9a**,**b** (Scheme 3). The stoichiometric quantities of 6-substituted pyrimidine thione derivatives **10a**,**b** and hydrazonoyl chlorides **4** or **5** were refluxed in a suitable amount of dioxane in the presence of Et_3N. Good yields (69%-81%) with high degree of purity of the products **13a-d** were obtained. The structure of the isolated triazolopyrimidines **13a-d** was confirmed based on the results obtained from their spectroscopic analyzes. We selected two charts of spectra one ^{1}H NMR of compound **13b** (Figure 1) and one ^{13}C NMR of derivative **13d** (Figure 2) to discuss their structures. ^{1}H NMR of triazolopyrimidine derivative **13b** showed three signals for $3CH_3$ groups with the expected splitting and one quartet signal for CH_2 of ester-CH_2CH_3 group, in addition to the presence of the pyrimidine-5-H as well as the three signals for aromatic-H(s).

^{13}C NMR is an excellent tool to prove the structure of the triazolopyrimidine derivatives **13a-d**. As an example for the prepared series **13a-d**, ^{13}C NMR of derivative **13d** (Figure 2) showed six splitted carbons due to the coupling between fluoride and carbon atoms at $\delta = 14.3$ (CH_3, dd, ^{3}JCF, 3 Hz), 108.0 (dd, ^{2}JCF, 28 Hz), 116.8 (dd, ^{3}JCF, 3 Hz), 124.2 (dd, ^{2}JCF, 17 Hz), 132.0 (dd, ^{3}JCF, 6 Hz), and 159.4 (dd, ^{1}JCF, 243 Hz).[40] Also, the appearance of a carbon signal of the amidic CO at $\delta = 162.9$ (C═O) ppm proved the cyclization of compounds **13** on the amidic nitrogen N3 not on the N1 in the pyrimidine ring.[11,34]

Under the same reaction condition, perimidine-2-thione **14** was reacted with each of the fluorinated

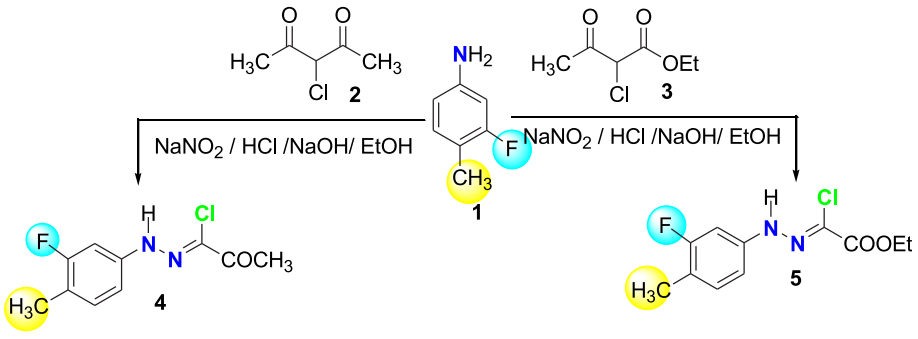

SCHEME 1 Synthesis of hydrazonoyl chlorides **4** and **5** [Colour figure can be viewed at wileyonlinelibrary.com]

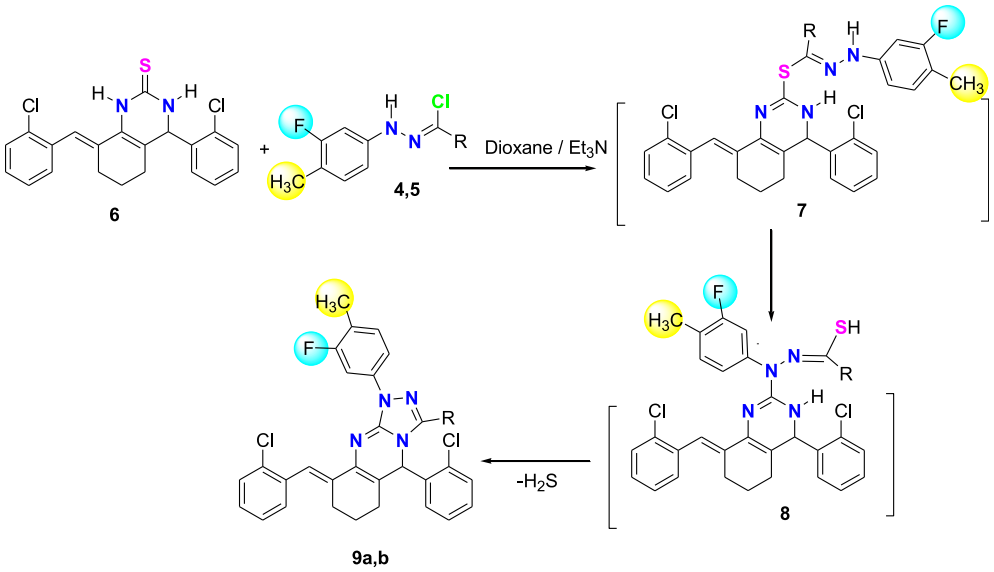

SCHEME 2 Synthesis of triazolopyrimidines **9a**,**b** [Colour figure can be viewed at wileyonlinelibrary.com]

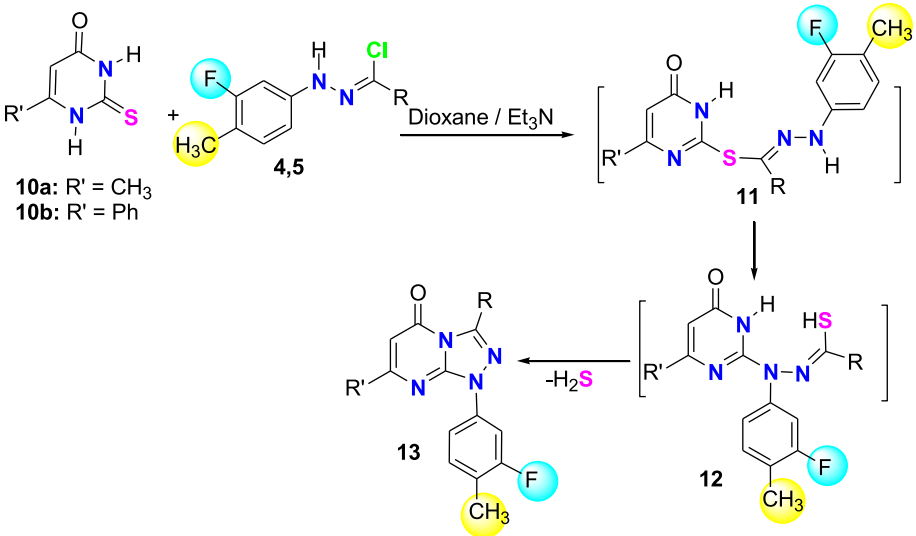

SCHEME 3 Synthesis of triazolopyrimidine derivatives **13a-d** [Colour figure can be viewed at wileyonlinelibrary.com]

hydrazonoyl chloride **4** and **5** in dioxane/Et_3N under reflux through the two intermediates **15** and **16** followed by cyclization to afford triazolo[4,3-*a*]perimidines **17a**,**b** (Scheme 4). Moreover, derivatives **19** and **21a**,**b** were obtained from the reaction of the two hydrazonoyl chlorides **4** and **5** with 1,8-diaminonaphthalene **18** and ketene aminal derivatives **20a**,**b** (Scheme 5). All the chemical structures of the synthesized products **17a**,**b**, **19**, and **21a**,**b** were confirmed based on the corrected data, which were extracted from their spectra (NMR, Mass, IR). For example, the mass spectra of all derivatives **17a**,**b**, **19**, and **21a**,**b** showed correct molecular ion peaks at the expected molecular weight for each derivative and all elemental analyses in the expected range as the calculated numbers. Furthermore, the IR spectra of derivatives **21a**,**b** revealed the absorption bands for the 2NH and 2C═O groups near 3400, 3154, 1690, and 1648 cm^{-1}.

Another valuable synthon is 4-amino-5-trifluoromethyl-4*H*-[1,2,4]triazole-3-thiol **22** reacted with hydrazonoyl chlorides **4** and **5** under the same reaction conditions as the previous reactions thermally at room temperature (Scheme 6). The reaction of aminotriazole thione derivative **22** when reacted with hydrazonoyl chloride **4** under reflux afforded triazolothiadiazine derivative **25**. When it reacted with hydrazonoyl chloride **5** under stirring at room temperature, it gave rich nitrogen molecule **27**. The structures of the two derivatives **25** and **28** were assured based on their IR, Mass, and ^1H NMR. The IR of derivative 25 was found to be free from any absorption band in the

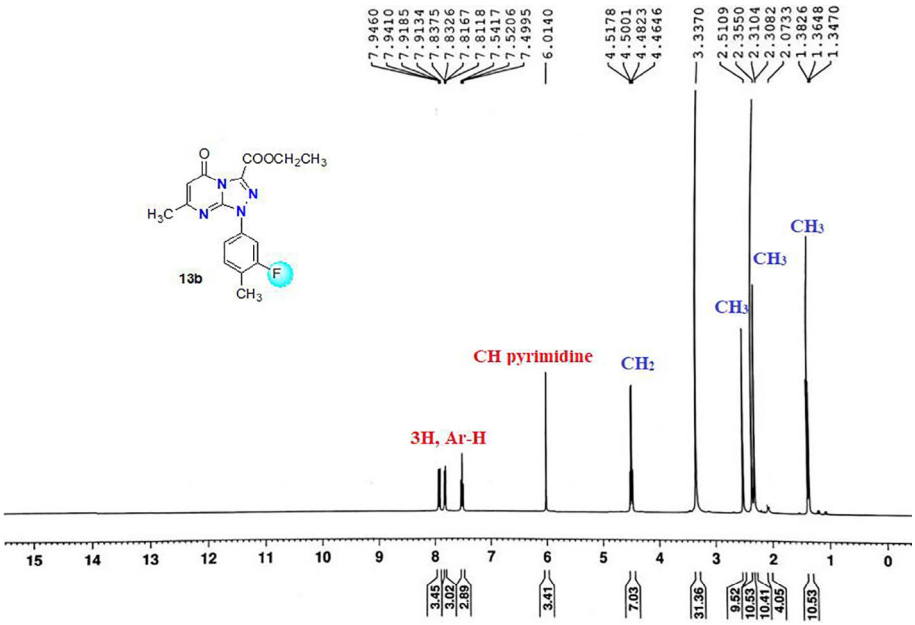

FIGURE 1 The ^{1}H NMR of compound **13b** [Colour figure can be viewed at wileyonlinelibrary.com]

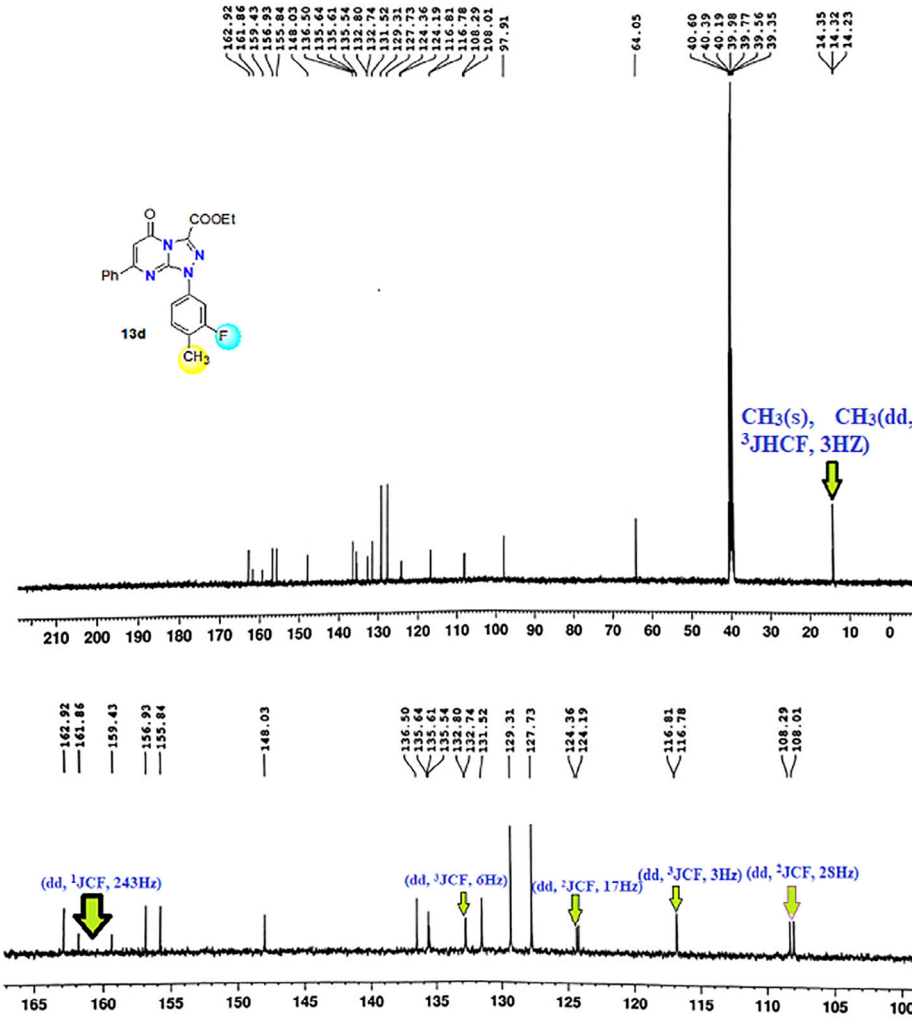

FIGURE 2 The ^{13}C NMR of compound **13d** [Colour figure can be viewed at wileyonlinelibrary.com]

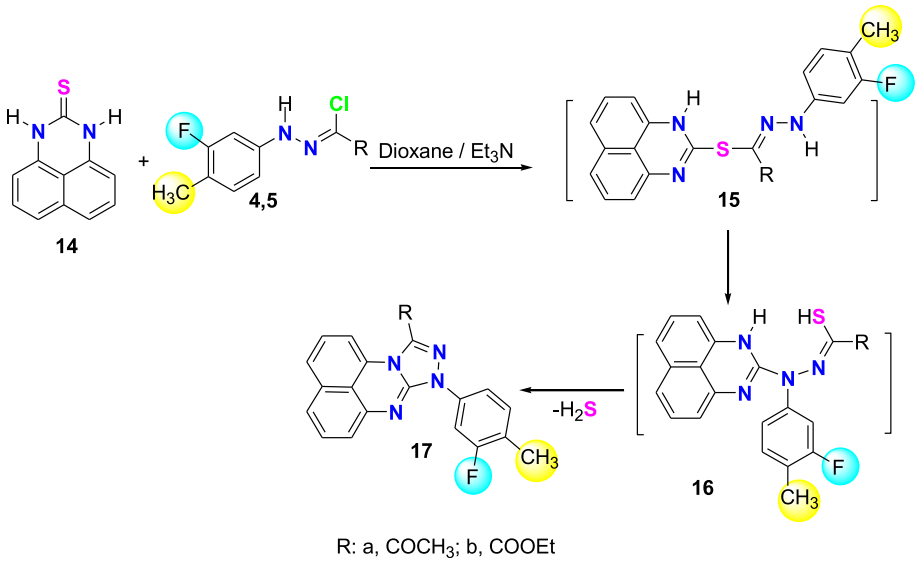

SCHEME 4 Synthesis of triazoloperimidine derivatives **17a**,**b** [Colour figure can be viewed at wileyonlinelibrary.com]

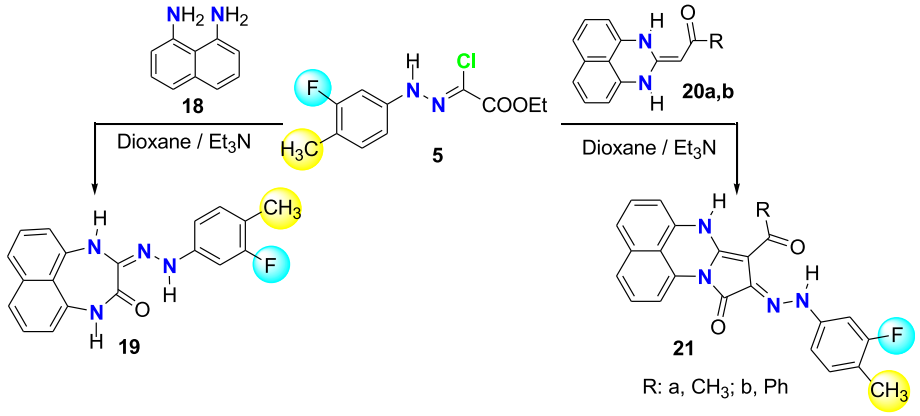

SCHEME 5 Reaction of hydrazonoyl chloride **5** with 1,8-diaminonaphthalene **18** and perimidine derivatives **20a**,**b** [Colour figure can be viewed at wileyonlinelibrary.com]

carbonyl group region (ν = 1630–1800 cm^{-1}). However, in the case of compound **28**, its IR spectrum has sharp absorption band at ν = 1736 cm^{-1} for the ester carbonyl group. In addition, the mass spectra for each compound **25** and **28** showed molecular ion peaks at the expected values corresponding to the suggested structures in Scheme 6.

2.1 | Antimicrobial activity

Antifungal and antibacterial activities of the target compounds were done at the Regional Center for Mycology and biotechnology (RCMB), Al-Azhar University, Cairo, Egypt. Compounds **4**, **5**, **9a**,**b**, **13a-d**, **17a**,**b**, **19**, **21a**,**b**, **25**, and **28** were examined for their *in vitro* antifungal, and antibacterial activities, by inhibition zone (IZ) technique. Two fungi: *Aspergillus flavus* (*A. flavus,* RCMB 002008) and *Candida albicans* (*C. albicans,* RCMB 005003), three Gram-positive bacteria, *Staphylococcus aureus* (*S. aureus,* RCMB 010010), *Bacillus subtilis* (*B. subtilis,* RCMB 015), *Enterococcus faecalis* (*E. faecalis*, ATCC 29212), and three Gram-negative bacteria: *Escherichia coli* (*E. coli,* RCMB 010052), *Proteus vulgaris* (*P. vulgaris,* RCMB 004), and *Enterobacter cloacae* (*E. cloacae*, RCMB 001), were used for this study compared to ketoconazole and gentamycin as reference antifungal and drugs antibacterial, respectively.

2.1.1 | Antifungal activity

The hydrazonoyl chlorides **4** and **5** revealed superior antifungal activities with IZ = 17 and 15 mm against *A. flavus* and 18 and 20 mm against *C. albicans*, respectively, compared to ketoconazole (IZ = 17 and 20 mm against *A. flavus* and *C. albicans*, respectively). Additionally, the triazolo thiadiazine derivative **25** exhibited potent antifungal activity (IZ = 15 and 18 mm against *A. flavus* and *C. albicans*, respectively). Moreover, the triazolopyrimidines **17a**,**b**, and dihydronaphtho diazepin-2(1*H*)-one derivative **19** displayed moderate activities with IZ values ranging from 9 to 14 mm.

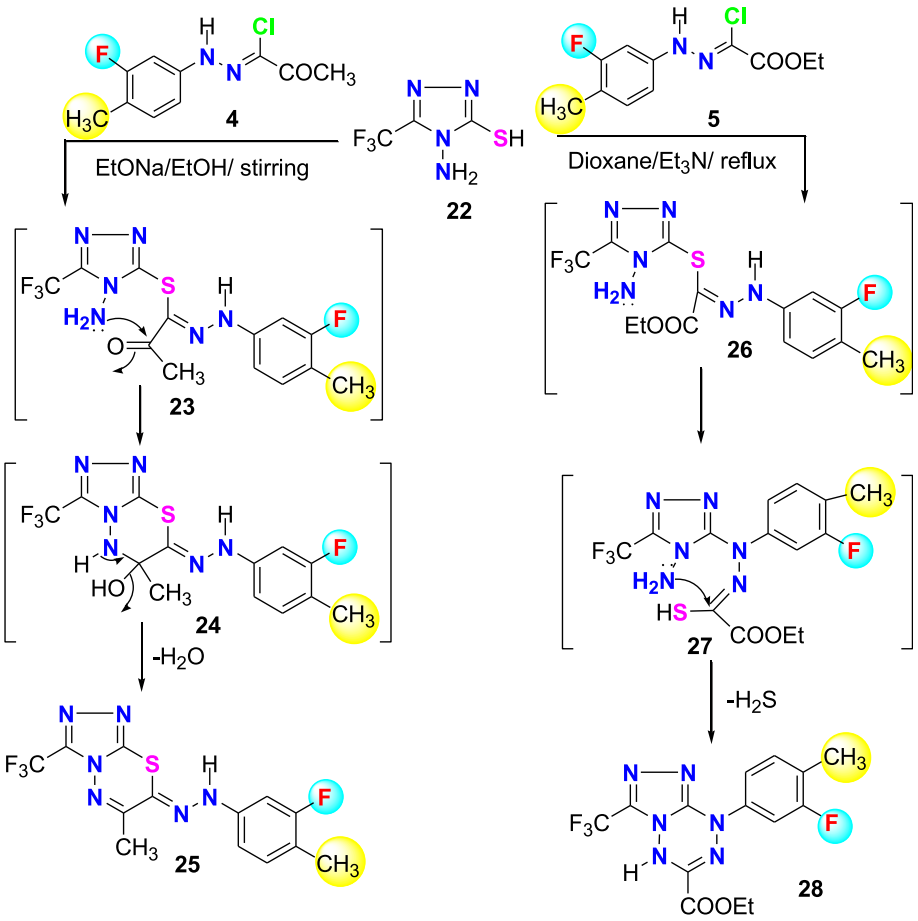

SCHEME 6 Reaction of hydrazonoyl chlorides **4** and **5** with 4-amino-5-trifluoromethyl-4*H*-[1,2,4] triazole-3-thiol **22** [Colour figure can be viewed at wileyonlinelibrary.com]

On the other hand, the triazolopyrimidines **9a**,**b**, and **13a-d** in addition to compounds **21a**,**b**, and **28** did not show any antifungal activities (Table 1).

2.1.2 | Antibacterial activity

Concerning the antibacterial activities of the synthesized compounds, moderate activities were observed for compounds **4** and **5** against most tested Gram-positive and Gram-negative bacterial strains showing IZ values at 13–25 mm. Regarding triazolopyrimidines **9a**,**b** and **13a-d**, no activity was seen against the Gram-positive *B. subtilis* or Gram-negative *E. coli,* while mild activities were noticed against *P. vulgaris* and *E. cloacae* with the exception of **9a** that was inactive against *E. cloacae*.

Furthermore, compound **19** showed moderate antibacterial activities against *E. faecalis* and *P. vulgaris* with IZ = 20 mm in comparison to gentamycin (IZ = 26 and 25 mm against *E. faecalis* and *P. vulgaris*, respectively). Also, compound **25** revealed moderate activity against *P. vulgaris* (IZ = 18 mm). The rest of the compounds displayed weak or no antibacterial activities (Table 2).

TABLE 1 Antifungal activity of the target compounds expressed as mean zones of inhibition (mm)

Compound	Tested fungi microorganisms	
	Aspergillus flavus	*Candida albicans*
4	17	18
5	15	20
9a	NA	NA
9b	NA	NA
13a	NA	NA
13b	NA	NA
13c	NA	NA
13d	NA	NA
17a	9	12
17b	10	14
19	13	14
21a	NA	NA
21b	NA	NA
25	15	18
28	NA	NA
Ketoconazole	17	20

TABLE 2 Antibacterial activity of the target compounds expressed as mean zones of inhibition (mm)

	Tested bacteria microorganisms					
	Gram-positive bacteria			*Gram-negative bacteria*		
Compound	***Staphylococcus aureus***	***Bacillus subtilis***	***Enterococcus faecalis***	***Escherichia coli***	***Proteus vulgaris***	***Enterobacter cloacae***
4	13	18	20	22	12	20
5	19	14	18	23	14	25
9a	NA	NA	12	NA	14	NA
9b	NA	NA	12	14	12	NA
13a	11	NA	NA	10	9	NA
13b	NA	NA	12	14	12	NA
13c	12	NA	10	11	12	NA
13d	13	NA	11	13	14	NA
17a	NA	NA	13	NA	15	12
17b	NA	NA	11	13	12	NA
19	15	15	20	11	20	16
21a	NA	NA	11	12	13	NA
21b	NA	NA	10	10	15	NA
25	NA	14	16	NA	18	15
28	12	11	13	NA	15	8
Gentamycin	24	26	26	30	25	30

As a general talk, we can conclude that the hydrazonoyl chlorides **4** and **5** showed the best antimicrobial activities among the tested compounds and that cyclization of the hydrazonoyl chloride moiety with different cyclic systems did not improve the activity.

2.2 | Molecular docking study

2.2.1 | Docking into leucyl-tRNA synthetase

Leucyl-tRNA synthetase (LeuRS) is a member of the aminoacyl tRNA synthetases family. It plays a critical role in the synthesis of protein of the microorganism, and thus essential for its survival, making this enzyme an attractive antimicrobial target.[41] Many recent studies in the literature have discussed the significance of aminoacyl tRNA synthetases family in developing antifungal and antibacterial agents.[42–45]

Here, we performed molecular docking study of compounds **4, 5, 17a**,**b**, **19**, and **25**, with significant antifungal activities, into the editing domain of *Candida albicans* cytosolic leucyl-tRNA synthetase (PDB code: 2WFG) to analyze their binding mode and affinity using MOE 2014 program.

Analysis of the docking simulation results (Table 3, Figures 3-8) revealed good fitting in the active site with docking scores from −5.014 to −6.851 kcal/mol, forming different types of interactions as hydrogen bond, π–cation, π–H, and hydrophobic interactions. All docked compounds formed interaction with the key amino acid residue Leu317 either through hydrogen bond or π–H interaction. The carbonyl group of the hydrazonoyl chlorides **4** and **5** interacted through H-bond with Leu317, while their phenyl moieties interacted through arene–cation interactions with Lys483 and Lys407, respectively. Also, the carbonyl group of **17a** was responsible for hydrogen bonding with Leu317, and the triazoloperimidine group formed two arene–H interactions with Lys483. On the other hand, triazoloperimidine moiety of compound **17b** was oriented in close contact with Leu317 forming arene–H interaction, however the ester oxygen was involved in hydrogen bonding with Lys483. Additional π–cation interaction was observed between the triazolo moiety of **17b** and Lys483.

Regarding the binding mode of the dihydronaphtho diazepin-2(1*H*)-one derivative **19**, arene–H interaction was formed between the diazepine and Leu317. Two hydrogen bonds were also seen, one is formed between the carbonyl oxygen and Thr316 and the second is between the hydrazono nitrogen and Lys483. Furthermore, compound

TABLE 3 Docking results of compounds **4**, **5**, **17a**,**b**, **19**, and **25** against *Candida albicans* leucyl-tRNA synthetase

Compound	Docking score (kcal/mol)	Interacting residues (Type of interaction)	Distance (A°)
4	−6.290	Leu317 (H bond) Lys483(π–cation)	3.16 3.64
5	−6.851	Leu317 (H-bond) Lys407 (π–cation)	3.05 3.86
17a	−5.014	Leu317 (H-bond) Lys483(π–H)	2.64 3.50, 4.80
17b	−6.234	Leu317 (π–H) Lys483(H bond) Lys483(π–cation)	3.84 2.42 4.02
19	−6.288	Thr316 (H bond) Leu317 (π–H) Lys483(H-bond)	3.19 4.40 2.88
25	−6.567	Leu317 (H-bond) Lys407 (π–H)	3.34 3.70

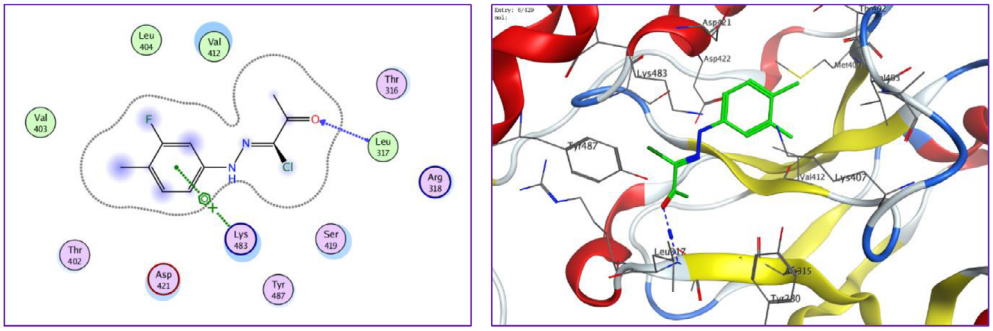

FIGURE 3 The 2D and 3D proposed binding modes of **4** docked in the active site of *Candida albicans* leucyl-tRNA synthetase [Colour figure can be viewed at wileyonlinelibrary.com]

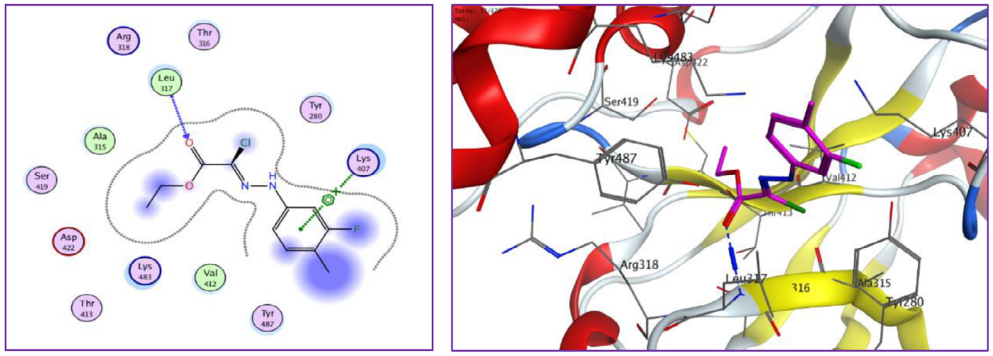

FIGURE 4 The 2D and 3D proposed binding modes of **5** docked in the active site of *Candida albicans* leucyl-tRNA synthetase [Colour figure can be viewed at wileyonlinelibrary.com]

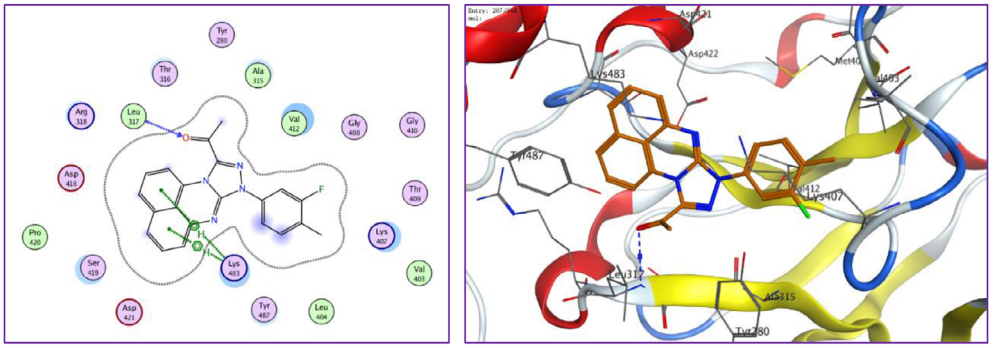

FIGURE 5 The 2D and 3D proposed binding modes of **17a** docked in the active site of *Candida albicans* leucyl-tRNA synthetase [Colour figure can be viewed at wileyonlinelibrary.com]

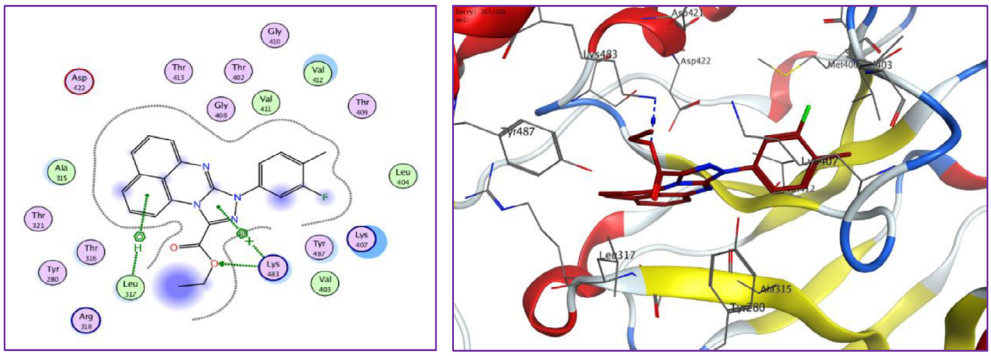

FIGURE 6 The 2D and 3D proposed binding modes of **17b** docked in the active site of *Candida albicans* leucyl-tRNA synthetase [Colour figure can be viewed at wileyonlinelibrary.com]

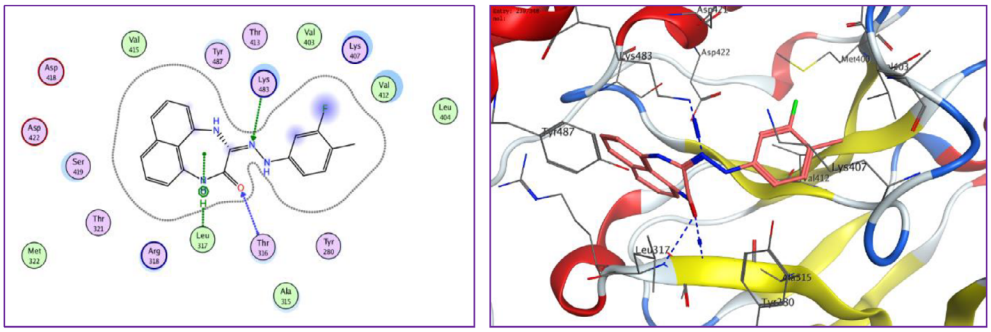

FIGURE 7 The 2D and 3D proposed binding modes of **19** docked in the active site of *Candida albicans* leucyl-tRNA synthetase [Colour figure can be viewed at wileyonlinelibrary.com]

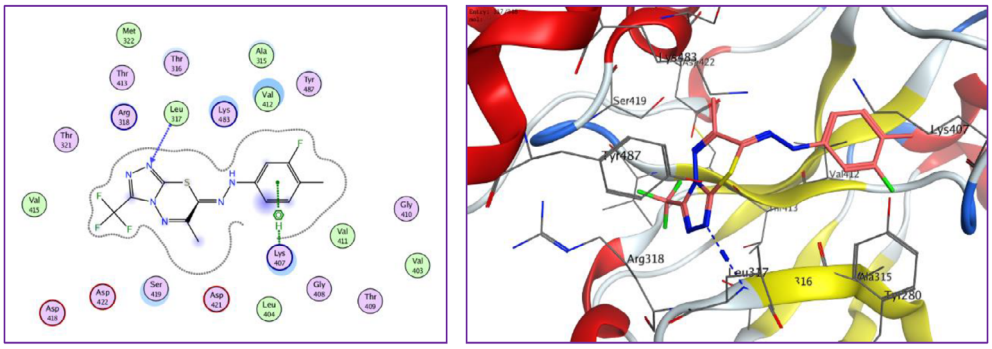

FIGURE 8 The 2D and 3D proposed binding modes of **25** docked in the active site of *Candida albicans* leucyl-tRNA synthetase [Colour figure can be viewed at wileyonlinelibrary.com]

25 displayed docking score of −6.567 Kcal/mol and showed similar binding mode to the hydrazonoyl **5**; the phenyl group interacted with Lys407, while the triazolo nitrogen interacted with Leu317 residue through hydrogen bond.

2.2.2 | Docking into COVID-19 3CLpro-2

The 3CLpro-2, the main protease of SARS-CoV-2, is vital in the maturation and replication process of the SARS-CoV-2, making it an important target for discovering new anti-coronavirus drugs.[18]

The structure of the 3CLprotease enzyme comprises three distinctive domains (Domain I, Domain II, and Domain III) made of 13 β-strands and 9 α-helices. In addition, there is a catalytic dyad in its structure formed of the conserved His41 and Cys145 residues, while the main site for substrate-binding appears as splitting between Domains I and II.[46]

To predict the binding mode and affinity of compounds **4**, **5**, **9a**,**b**, **13a-d**, **17a**,**b**, **19**, **21a**,**b**, **25**, and **28** into the binding site of COVID-19 3CLpro (PDB: 6LU7), molecular docking simulation was performed. As represented in Table 4, most of the tested compounds fit properly in the COVID-19 3CL protease active site with binding energies ranging from −5.510 to −7.529 kcal/mol. Generally, all of the compounds, with the exception of **9a**, formed hydrogen bond interaction with the key amino acid Cys145. Besides, residues Asn142, Gly143, Ser144, His163, His164, and Gln189 were also contributed in hydrogen bonding. While His41, Gly143, Met165, and Gln189 were involved in π–H interactions.

TABLE 4 Docking results of the target compounds against COVID-19 3CLpro

Compound	Docking score (kcal/mol)	Interacting residues (Type of interaction)	Distance (A^0)
4	−7.158	Cys145 (H bond) His164 (H bond)	4.10 2.92
5	−7.529	Asn142(H bond) Cys145 (H bond) His164 (H bond)	3.10, 3.39 3.49 2.74, 2.93
9a	−5.510	—	—
9b	−5.670	Cys145 (H bond) His163 (H bond)	4.00 2.62
13a	−6.153	Gly143(H bond) Ser144 (H bond) Cys145 (H bond)	2.82 2.86 3.27
13b	−6.280	Ser144 (H bond) Cys145 (H bond)	2.82 3.29, 3.85
13c	−6.945	His41 (H–π) Gly143(H bond) Cys145 (H bond)	4.04 3.13 4.21
13d	−7.239	His41 (H–π) Gly143(H bond) Cys145 (H bond)	4.08 3.29 4.06
17a	−6.746	Cys145 (H bond) His163 (H bond)	3.44, 3.62 2.87
17b	−6.657	Cys145 (H bond)	3.31
19	−6.116	Cys145 (H bond) His164 (H bond)	3.49, 4.04 2.89
21a	−6.253	Gly143 (π–H) Cys145 (H bond) Gln189 (π–H)	3.89 4.27 4.46
21b	−6.827	Cys145 (H bond) Gln189 (H bond)	3.49 3.03
25	−7.517	Cys145 (H bond) His163 (H bond) His164 (H bond) Met165(π–H)	4.13 3.05 2.98 4.98
28	−6.471	Gly143 (H bond) Cys145 (H bond)	2.80 3.25

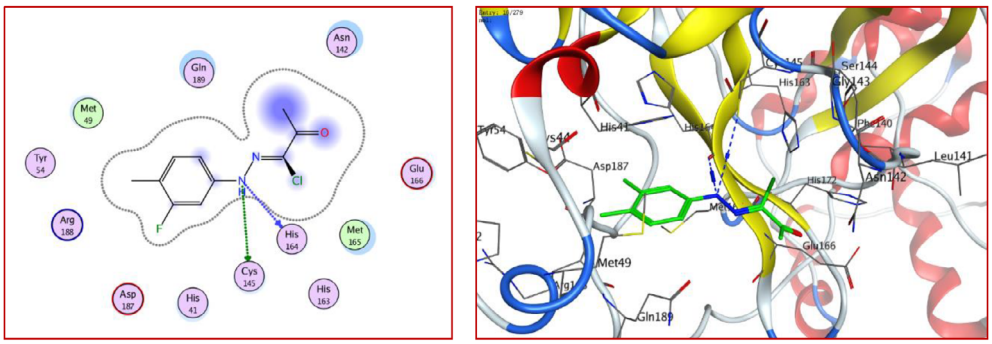

FIGURE 9 The 2D and 3D proposed binding modes of **4** docked in the active site of COVID-19 3CLpro [Colour figure can be viewed at wileyonlinelibrary.com]

Focusing on the mode of binding of the hydrazonoyl chlorides **4** and **5**, strong binding with docking score values of −7.158 and −7.529 Kcal/mol, respectively, were observed. As shown in **Figures 9** and **10**, hydrogen bond interactions were formed between the hydrazono NH groups of **4**/**5** and both Cys145 and His164 residues. Another hydrogen bonds were noticed between the ester group of **5** and Asn142. Also, the triazolopyrimidine derivatives **13c** and **13d** could fit well in the active site (docking score −6.954 and −7.239 Kcal/mol, respectively). One of their triazolo nitrogen atoms formed hydrogen bond with Gly143, while the acetyl/ester carbonyl groups were involved in hydrogen bonding with the important Cys145 residue. Moreover, the phenyl groups of **13c** and **13d** were found to form H–π interactions with His41 (**Figures 11** and **12**).

Concerning the triazolo thiadiazine derivative **25**, the hydrazono NH group was responsible for the hydrogen bonding with Cys145 and His164, while the triazolo nitrogen atom formed hydrogen bond with His163. Besides, π–H interaction was seen between the triazolo thiadiazine moiety and Met165 as displayed in Figure 13.

3 | CONCLUSION

Ultimately, this research article contains valuable diverse azoloazine derivatives that we synthesized from the reaction of two fluorinated hydrazonoyl chlorides with heterocyclic thiones, 1,8-diaminonaphthalene, ketenaminal derivative, and 4-amino-5-triflouromethyl-1,2,4-triazole-2-thiol. The mechanistic pathways and the structures of all synthesized derivatives were discussed and assured based on the available spectral data. The antimicrobial evaluation of the target compounds revealed that the hydrazonoyl chlorides **4** and **5** were the most active as antimicrobials among the tested compounds. Additionally, compounds **17a**,**b**, **19**, and **25**

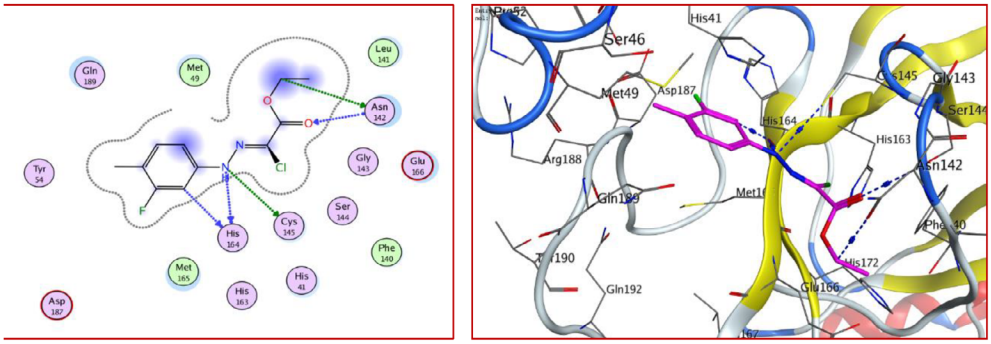

FIGURE 10 The 2D and 3D proposed binding modes of **5** docked in the active site of COVID-19 3CLpro [Colour figure can be viewed at wileyonlinelibrary.com]

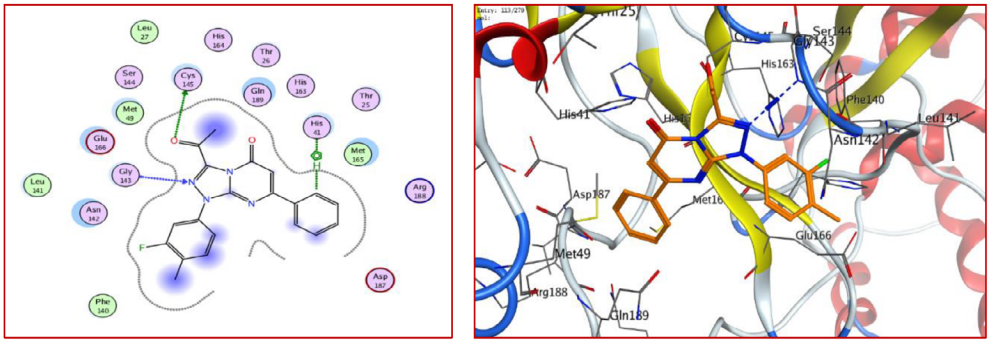

FIGURE 11 The 2D and 3D proposed binding modes of **13c** docked in the active site of COVID-19 3CLpro [Colour figure can be viewed at wileyonlinelibrary.com]

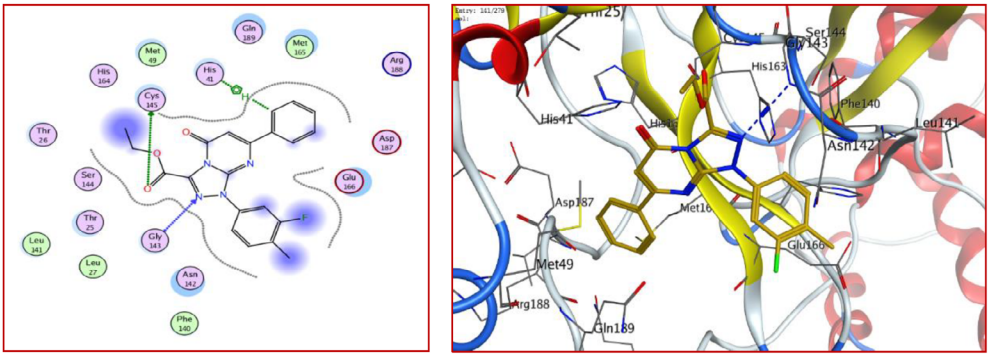

FIGURE 12 The 2D and 3D proposed binding modes of **13d** docked in the active site of COVID-19 3CLpro [Colour figure can be viewed at wileyonlinelibrary.com]

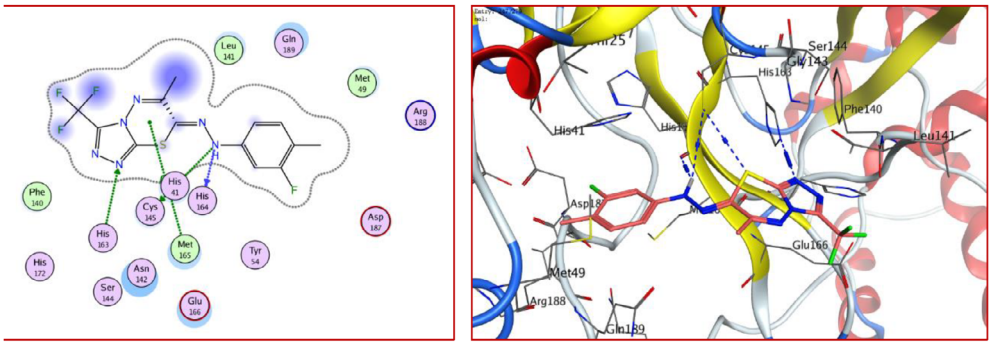

FIGURE 13 The 2D and 3D proposed binding modes of **25** docked in the active site of COVID-19 3CLpro [Colour figure can be viewed at wileyonlinelibrary.com]

exhibited promising antifungal activities. Molecular modeling simulation showed that compounds **4**, **5**, **17a**,**b**, **19**, and **25** could fit properly to *C. albicans* leucyl-tRNA synthetase active site. As well, docking study into the COVID-19 3CL protease active site displayed well-fitting of most of the synthesized compounds with docking score values from −5.510 to −7.529 kcal/mol, suggesting the possibility of these compounds to act as antivirals against SARS-COV-2.

3.1 | Experimental

Melting points of all new isolated heterocyclic derivatives **9a**,**b**, **13a-d**, **17a**,**b**, **19**, **21a**,**b**, **25**, **and 28** were detected on a Gallenkamp device without correction. IR spectra of these derivatives **9a**,**b**, **13a-d**, **17a**,**b**, **19**, **21a**,**b**, **25**, **and 28** were determined after converted to disc with potassium bromide using spectrophotometer (Pye-Unicam SP300). Moreover, solution of deuterated DMSO-d_6 was used to determine the spectra of ^{1}H and ^{13}C NMR on a Varian Gemini 300 NMR spectrometer (400 MHz for ^{1}H NMR and 100 MHz for ^{13}C NMR) and the two chemical shifts values at δ: 2.5 and 3.3 ppm were corresponding to the utilized solvent (DMSO-d_6). Mass spectra for all synthesized derivatives were recorded on a GCMS-Q1000-EX Shimadzu and GCMS 5988-A HP spectrometers, the ionizing voltage was 70 eV. Elemental analyses of the products were carried out at the Microanalytical Centre of Cairo University, Giza, Egypt. The biological evaluation of the products was carried out at Regional Center for Mycology and Biotechnology at Al-Azhar University, Cairo, Egypt. The two fluorinated hydrazonoyl chlorides were prepared according to our literature report.[38]

3.2 | Reaction of fluorinated hydrazonoyl chlorides 4 and 5 with pyrimidine thione derivatives 6, 10, 14 and with 1,8-dinaphthylamine 18 and ketene aminal derivatives 20a,b

The method of synthesis of all triazolopyrimidines **9a**,**b**, **13**, **17** and napthodiazepine **19** and pyridopyrimidines **21a**,**b** was proceeded by the same manner as follows: in suitable round flask, we added equal amounts of compounds **6**, **10**, **14**, **18**, or **20a**,**b** and the fluorinated hydrazonoyl chlorides **4** or **5** (1 mmol of each) in 20 mL dioxane. This flask was subjected to reflux till all solid dissolve, and then we added the equivalent amount of Et_3N (0.3 mL), and the reaction was completed after 10 hours reflux. The colored solid formed was collected and washed with water then crystallized from ethanol/dioxin mixture to afford the derivatives **9a**,**b**, **13a-d**, **17a**,**b**, **19**, and **21a**,**b**.

3.3 | 3-Acetyl-9-(2-Chlorobenzylidene)-5-(2-chlorophenyl)-1-(3-fluoro-4-methylphenyl)-1,5,6,7,8,9-hexahydro-[1,2,4]triazolo[3,4-b]quinazoline (9a)

Yellow solid, 71% yield; mp. 185 to 186°C; IR (KBr): ν 3083 (sp^2 C—H), 2918 (sp^3 C—H), 1698 (C═O), 1639 (C═N), 1539, 1464, 1437, 1387, 1327, 1264, 1171, 1135 cm^{-1}; ^{1}H NMR (DMSO-d_6): δ 1.14–2.24 (m, 6H, 3CH_2), 2.41 (s, 3H, CH_3), 2.56 (s, 3H, $COCH_3$), 6.65 (s, 1H, CH quinazolin-H), 7.16–7.50 (m, 9H, Ar-H), 7.56 (s, 1H, ═CH), 7.99 (dd, J = 2,11 *Hz*, 1H Ar-H), 8.34 (dd, J = 2,11 *Hz*, 1H Ar-H). MS m/z (%): 559 (M^+, 10), 421 (48), 387 (22), 353 (41), 343 (53), 325 (59), 262 (42), 252 (100), 237 (49), 233 (84), 179 (76). Anal. Calcd for $C_{31}H_{25}Cl_2FN_4O$ (559.47): C, 66.55; H, 4.50; N, 10.01. Found: C, 66.62; H, 4.41; N, 9.89%.

3.4 | Ethyl 9-(2-chlorobenzylidene)-5-(2-chlorophenyl)-1-(3-fluoro-4-methylphenyl)-1,5,6,7,8,9-hexahydro-[1,2,4]triazolo[3,4-b]quinazoline-3-carboxylate (9b)

Yellow solid, 78% yield; mp. 192 to 194°C; IR (KBr): ν 3061, 2927 (C—H), 1724 (C═O), 1605 (C═N), 1534, 1432, 1337, 1243, 1176 cm^{-1}; MS m/z (%): 591 (M^++2, 41), 590 (M^++1, 31), 589 (M^+, 60), 545 (53), 502 (54),

490 (58), 469 (100), 427 (35), 336 (79), 325 (60), 251 (58), 176 (38), 152 (51), 81 (52). Anal. Calcd for $C_{32}H_{27}Cl_2FN_4O_2$ (589.49): C, 65.20; H, 4.62; N, 9.50. Found: C, 65.38; H, 4.58; N, 9.42%.

3.5 | 3-Acetyl-1-(3-fluoro-4-methylphenyl)-7-methyl-[1,2,4]triazolo [4,3-a]pyrimidin-5(1H)-one (13a)

Yellow solid, 78% yield; mp. 240 to 242°C; IR (KBr): ν 3031 (sp^2 C—H), 2928 (sp^3 C—H), 1676, 1629 (2C═O), 1515, 1423, 1311, 1265, 1195, 1054 cm^{-1}; ^1H NMR (DMSO-d_6): δ 2.28 (s, 3H, CH_3), 2.35 (s, 3H, CH_3), 2.70 (s, 3H, $COCH_3$), 6.02 (s, 1H, pyrimidine-H), 7.48 (t, J = 6 Hz, 1H, Ar-H), 7.85 (dd, J = 2.8, 11.2 Hz, 1H, Ar-H), 7.9 (dd, J = 2.8, 11.2 Hz, 1H, Ar-H). MS m/z (%): 302 (M^++2, 58), 300 (M^+, 9), 289 (40), 265 (65), 243 (54), 213 (93), 167 (38), 143 (100), 89 (37). Anal. Calcd for $C_{15}H_{13}FN_4O_2$ (300.29): C, 60.00; H, 4.36; N, 18.66. Found: C, 60.21; H, 4.26; N, 18.53%.

3.6 | Ethyl 1-(3-fluoro-4-methylphenyl)-7-methyl-5-oxo-1,5-dihydro-[1,2,4]triazolo [4,3-a]pyrimidine-3-carboxylate (13b)

White solid, 69% yield; mp. 170 to 172°C; IR (KBr): ν 3090 (sp^2 C—H), 2996 (sp^3 C—H), 1750, 1705 (2C═O), 1597, 1578, 1515, 1455, 1291, 1172, 1120 cm^{-1}; ^1H NMR (DMSO-d_6): δ 1.35 (t, J = 7 Hz, 3H, CH_3), 2.31 (s, 3H, CH_3), 2.51 (s, 3H, CH_3), 4.46 (q, J = 7 Hz, 2H, CH_2), 6.01 (s, 1H, pyrimidine-H), 7.49 (t, J = 8 Hz, 1H, Ar-H), 7.8 (dd, J = 2, 11 Hz, 1H, Ar-H), 7.91 (dd, J = 2, 11 Hz, 1H, Ar-H). Anal. Calcd for $C_{16}H_{15}FN_4O_3$ (330.31): C, 58.18; H, 4.58; N, 16.96. Found: C, 58.26; H, 4.45; N, 16.86%.

3.7 | 3-Acetyl-1-(3-fluoro-4-methylphenyl)-7-phenyl-[1,2,4]triazolo [4,3-a]pyrimidin-5(1H)-one (13c)

Yellow solid, 77% yield; mp. 210 to 212°C; IR (KBr): ν 3069 (sp^2 C—H), 2978 (sp^3 C—H), 1676, 1625 (2C═O), 1590, 1457, 1376, 1361, 1265, 1173, 1109 cm^{-1}; ^1H NMR (DMSO-d_6): δ 2.20 (s, 3H, CH_3), 2.47 (s, 3H, CH_3), 6.30 (s, 1H, CH-pyrimidine-H), 7.29–7.79 (m, 8H, Ar-H); MS m/z (%): 364 (M^++2, 10), 362 (M^+, 29), 354 (72), 341 (100), 317 (71), 289 (90), 280 (81), 253 (60), 237 (72), 224 (40), 161 (34), 104 (25), 71 (47). Anal. Calcd for $C_{20}H_{15}FN_4O_2$ (362.36): C, 66.29; H, 4.17; N, 15.46. Found: C, 66.38; H, 4.06; N, 15.35%.

3.8 | Ethyl 1-(3-fluoro-4-methylphenyl)-5-oxo-7-phenyl-1,5-dihydro-[1,2,4]triazolo [4,3-*a*] pyrimidine-3-carboxylate (13d)

White solid, 81% yield; mp. 180 to 182°C; IR (KBr): ν 3086 (sp^2 C—H), 2986 (sp^3 C—H), 1748, 1697 (2C═O), 1600, 1575, 1485, 1387, 1274, 1181, 1102 cm^{-1}; ^1H NMR (DMSO-d_6): δ 1.38 (t, J = 7.12 Hz, 3H, CH_3), 2.33 (s, 3H, CH_3), 4.49 (q, J = 7.12 Hz, 2H, CH_2), 6.73 (s, 1H, pyrimidine-H), 7.55–8.16 (m, 8H, Ar-H); ^{13}C NMR (DMSO-d_6): δ 14.2 (CH_3), 14.3 (CH_3, dd, ^{3}JCF, 3 Hz), 64.1 (CH_2), 97.9, 108.0 (dd, ^{2}JCF, 28 Hz), 116.8 (dd, ^{3}JCF, 3 Hz), 124.2 (dd, ^{2}JCF, 17 Hz), 127.7, 129.3, 131.5, 132.0 (dd, ^{3}JCF, 6 Hz), 135.5, 135.6, 136.5, 148.0, 155.8, 156.9 (C═O ester), 159.4 (dd, ^{1}JCF, 243 Hz), 162.9 (C═O); MS m/z (%): 392 (M^+, 21), 380 (54), 248 (54), 272 (45), 251 (78), 180 (29), 137 (74), 133 (100), 131 (83), 71 (43). Anal. Calcd for $C_{21}H_{17}FN_4O_3$ (392.39): C, 64.28; H, 4.37; N, 14.28. Found: C, 64.48; H, 4.24; N, 14.09%.

3.9 | 1-(8-(3-Fluoro-4-methylphenyl)-8H-[1,2,4]triazolo[4,3-a]perimidin-10-yl)ethan-1-one (17a)

Orange solid, 70% yield; mp. 235 to 237°C; IR (KBr): ν 3086, 3052 (sp^2 C—H), 2974 (sp^3 C—H), 1709 (C═O), 1643, 1618 (C═N), 1588, 1542, 1453, 1368, 1259, 1202, 1118, 1076 cm^{-1}; ^1H NMR (DMSO-d_6): δ 2.18 (s, 3H, CH_3), 2.53 (s, 3H, $COCH_3$), 6.73–8.07 (m, 9H, Ar-H); MS m/z (%): 359 (M^++1, 7), 358 (M^+, 48), 353 (45), 351 (35), 318 (59), 303 (57), 286 (100), 256 (67), 228 (69), 197 (44), 186 (64), 120 (71), 115 (60), 102 (48). Anal. Calcd for $C_{21}H_{15}FN_4O$ (358.37): C, 70.38; H, 4.22; N, 15.63. Found: C, 70.46; H, 4.04; N, 15.52%.

3.10 | Ethyl 8-(3-fluoro-4-methylphenyl)-8*H*-[1,2,4]triazolo[4,3-*a*]perimidine-10-carboxylate (17b)

Orange solid, 76% yield; mp. 215 to 217°C; IR (KBr): ν 3085, 3051 (sp^2 C—H), 2981 (sp^3 C—H), 1736 (C═O), 1639, 1622 (C═N), 1585, 1446, 1417, 1369, 1267, 1209, 1180, 1079 cm^{-1}; ^1H NMR (DMSO-d_6): δ 1.38 (t, J = 9 Hz, 3H, CH_3), 2.26 (s, 3H, CH_3), 4.50 (q, J = 9 Hz, 2H, CH2), 6.75 (d, G = 8 Hz, 1H, naphthalene-H), 7.09–7.46 (m, 6H, Ar-H), 7.08 (dd, J = 2, 11 Hz, 1H, Ar-H), 7.96 (d, J = 8 Hz, 1H, nathalene-H). ^{13}C NMR (DMSO-d_6): δ 14.3 (CH_3), 14.4 (CH_3, dd, ^{3}JCF, 3 Hz), 63.9 (CH_2), 106.7 (dd, ^{2}JCF, 28 Hz), 107.4, 110.8, 114.7, 115.4 (dd, ^{3}JCF, 6 Hz), 118.7, 119.3, 120.3, 122.4, 123.5, 126.9, 129.2, 131.9 (dd, ^{2}JCF, 22 Hz), 135.5, 136.2 (dd, ^{3}JCF, 11 Hz),

143.2, 146.3, 157.3 (C═O ester), 159.4 (dd, ^{1}JCF, 241 Hz); MS *m/z* (%): 390 (M^++2, 20), 388 (M^+, 35), 371 (33), 317 (36), 279 (100), 250 (48), 189 (51), 154 (48), 99 (30). Anal. Calcd for $C_{22}H_{17}FN_4O_2$ (388.40): C, 68.03; H, 4.41; N, 14.43. Found: C, 68.16; H, 4.27; N, 14.28%.

3.11 | 3-(2-(3-Fluoro-4-methylphenyl) hydrazono)-3,4-dihydronaphtho[1,8-ef][1,4] diazepin-2(1H)-one (19)

Brown solid, 73% yield; mp. 155 to 157°C; IR (KBr): *ν* 3397 (br., 3NH), 3046 (sp^2 C—H), 2923 (sp^3 C—H), 1677 (C═O), 1629 (C═N), 1595, 1510, 1457, 1397, 1310, 1263, 1182, 1113 cm^{-1}; ^{1}H NMR (DMSO-d_6): *δ* 2.35 (s, 3H, CH_3), 7.10–7.89 (m, 9H, Ar-H), 8.80 (s, 1H, NH), 9.82 (s, 1H, NH), 11.78 (s, 1H, NH); MS *m/z* (%): 336 (M^++2, 43), 334 (M^+, 32), 328 (35), 321 (100), 316 (57), 311 (70), 296 (70), 288 (37), 278 (81), 228 (13), 210 (50), 188 (54), 168 (45), 138 (38), 110 (58). Anal. Calcd for $C_{19}H_{15}FN_4O$ (334.35): C, 68.25; H, 4.52; N, 16.76. Found: C, 68.39; H, 4.46; N, 16.66%.

3.12 | 8-Acetyl-9-(2-(3-fluoro-4-methylphenyl)hydrazono)-7,9-dihydro-10*H*-pyrrolo[1,2-*a*]perimidin-10-one (21a)

Orange solid, 70% yield; mp. 160 to 161°C; IR (KBr): *ν* 3432 (br., 2NH), 3058 (sp^2 C—H), 2922 (sp^3 C—H), 1678, 1648 (2C═O), 1619 (C═N), 1597, 1518, 1457, 1375, 1312, 1275, 1194, 1110 cm^{-1}; ^{1}H NMR (DMSO-d_6): *δ* 2.13 (s, 3H, CH_3), 3.51 (s, 3H, CH_3), 7.16–8.23 (m, 9H, Ar-H), 10.56 (br s, 2H, 2NH); MS *m/z* (%): 402 (M^+, 39), 400 (M^+, 29), 393 (34), 377 (100), 322 (67), 318 (77), 273 (88), 215 (35), 198 (55), 135 (35), 87 (55). Anal. Calcd for $C_{23}H_{17}FN_4O_2$ (400.41): C, 68.99; H, 4.28; N, 13.99. Found: C, 69.13; H, 4.06; N, 13.83%.

3.13 | 8-Benzoyl-9-(2-(3-fluoro-4-methylphenyl)hydrazono)-7,9-dihydro-10H-pyrrolo[1,2-a]perimidin-10-one (21b)

Orange solid, 76% yield; mp. 165 to 166°C; IR (KBr): *ν* 3433, 3154 (2NH), 2919 (sp^3 C—H), 1692, 1648 (2C═O), 1622 (C═N), 1575, 1469, 1402, 1374, 1273, 1192, 1109 cm^{-1}; ^{1}H NMR (DMSO-d6): δ 2.51 (s, 3H, CH_3), 7.22–8.77 (m, 14H, Ar-H), 10.85 (s, 1H, NH), 11.66 (s, 1H, NH); MS *m/z* (%): 462 (M^+, 9), 440 (8), 347 (10), 334 (10), 251 (100), 195 (32), 179 (38), 127 (16), 89 (31), 77 (30). Anal. Calcd for $C_{28}H_{19}FN_4O_2$ (462.48): C, 72.72; H, 4.14; N, 12.11. Found: C, 72.59; H, 4.04; N, 12.02%.

3.14 | Reaction of fluorinated hydrazonoyl chlorides 4 and 5 with 4-amino-5-trifluoromethyl-4*H*-[1,2,4] triazole-3-thiol (22)

The same number of moles (0.001 mole) of triazoleaminothione derivatives **22** was reacted with each of the fluorinated hydrazonoyl chlorides **4** or **5** in dioxane (20 mL) in basic medium (Et_3N, 0.3 mL) under continuous stirring overnight as in the case of compound **4** and under reflux for 10 h as in the case of compound **5**. After the reactions were completed (Monitored with TLC test), the formed solids were filtered and washed with H_2O, then crystalized from dioxane/ethanol mixture to afford the colored compounds **25** and **28**.

3.15 | 7-(2-(3-Fluoro-4-methylphenyl) hydrazono)-6-methyl-3-(trifluoromethyl)-7*H*-[1,2,4] triazolo[3,4-*b*][1,3,4] thiadiazine (25)

Yellow solid, 75% yield; mp. 190 to 192°C; IR (KBr): *ν* 3442 (NH), 3054 (sp^2 C—H), 2986 (sp3 C—H), 1626 (C═N), 1540, 1507, 1457, 1393, 1262, 1186, 1119 cm^{-1}; ^{1}H NMR (DMSO-d_6): *δ* 2.15 (s, 3H, CH_3), 2.49 (s, 3H, CH_3), 7.09–7.18 (m, 3H, Ar-H), 9.15 (s, 1H, NH); MS *m/z* (%): 360 (M^++2, 34), 358 (M^+, 100), 355 (68), 320 (35), 296 (72), 270 (86), 233 (75), 142 (83), 128 (94), 89 (85). Anal. Calcd for $C_{13}H_{10}F_4N_6$ (358.32): C, 43.58; H, 2.81; N, 23.45. Found: C, 43.65; H, 2.70; N, 23.28%.

3.16 | Ethyl 8-(3-fluoro-4-methylphenyl)-3-(trifluoromethyl)-5,8-dihydro-[1,2,4] triazolo[4,3-b][1,2,4,5]tetrazine-6-carboxylate (28)

Orange solid, 78% yield; mp. 200 to 202°C; IR (KBr): *ν* 3347 (NH), 2982 (sp^3 C—H), 1736 (C═O), 1626 (C═N), 1589, 1511, 1457, 1426, 1380, 1269, 1187, 1072 cm^{-1}; ^{1}H NMR (DMSO-d6): δ 1.18 (t, J = 7 Hz, 3H, CH_3), 2.33 (s, 3H, CH_3), 4.31 (q, J = 7 Hz, 2H, CH_2), 7.00–7.87 (m, 3H, Ar-H), 9.95 (s, 1H, NH); MS *m/z* (%): 374 (M^++2, 31), 372 (M^+, 35), 509 (42), 330 (71), 308 (36), 294 (46), 242 (76), 208 (41), 167 (89), 118 (40), 80 (65), 51 (100). Anal. Calcd for $C_{14}H_{12}F_4N_6O_2$ (372.28): C, 45.17; H, 3.25; N, 22.57. Found: C, 45.26; H, 3.11; N, 22.49%.

3.17 | Biological activity

The synthesized azoloazine derivatives **4**, **5**, **9a**,**b**, **13a-d**, **17a**,**b**, **19**, **21a**,**b**, **25**, and **28** were assayed in *vitro* for their antimicrobial activity using the agar diffusion method.[47] The activity of 30 μg/mL concentration of each azoloazine derivatives was investigated separately on each microorganism. The IZD diameter of the mm/mg azoloazine compounds is used as a standard for antimicrobial impact. Initially, using a sterile cotton swab, the microorganisms were spread uniformly on fresh Petri dishes with agar-agar and nutrient agar. One hundred μl of each sample was taken and added to each well (10 mm holes cut in an agar gel, 20 mm away from each other). At a temperature of 36°C, the Petri dishes were incubated for bacteria, and the fungi were incubated at 28°C. After about 24 hours of incubation, areas of inhibition were measured in millimeters. Each test was repeated three times and the average value was recorded. The fungicide amphotericin, gentamicin, and ampicillin were used as reference to evaluate the effectiveness of compounds tested under the same conditions. The results of the antimicrobial and antifungal effects test are summarized in Tables 1 and 2.

3.18 | Molecular docking

Molecular docking analysis was done by using MOE-Dock 2014 software.[48] Chemical structures of the tested compounds were sketched by the builder of the MOE and minimized using the program force field MMFF94x. Then, the protein was prepared, hydrogen atoms were added, and undesirable water molecules were removed. After that, docking of the 3D conformers was done; using rescoring 1(London dG) and rescoring 2 (GBVI/WSA dG). "Ligand Interactions" tool was utilized for the visualization of the 2D protein–ligand interactions, showing the different formed interactions.

DATA AVAILABILITY STATEMENT

The data that supports the findings of this study are available in the supplementary material of this article

ORCID

Zeinab A. Muhammad https://orcid.org/0000-0003-1711-8497
Thoraya A. Farghaly https://orcid.org/0000-0002-9620-8548

REFERENCES

[1] WHO Report on Surveillance of Antibiotic Consumption 2018. https://www.who.int/medicines/areas/rational_use/oms-amr-amc-report-2016-2018/en/
[2] D. Armstrong-James, G. Meintjes, G. D. Brown, *Trends Microbiol.* **2014**, *22*, 120. https://doi.org/10.1016/j.tim.2014.01.001.
[3] F. L. Rock, W. Mao, A. Yaremchuk, M. Tukalo, T. Crepin, H. Zhou, Y. K. Zhang, V. Hernandez, T. Akama, S. J. Baker, J. J. Plattner, L. Shapiro, S. A. Martinis, S. J. Benkovic, S. Cusack, M. R. Alley, *Science* **2007**, *316*, 1759. https://doi.org/10.1126/science.1142189.
[4] J. S. Pham, K. L. Dawson, K. E. Jackson, E. E. Lim, C. F. A. Pasaje, K. E. C. Turner, S. A. Ralph, *Int. J. Parasitol Drugs Drug Resis.* **2014**, *4*, 1. https://doi.org/10.1016/j.ijpddr.2013.10.001.
[5] E. Seiradake, W. Mao, V. Hernandez, S. J. Baker, J. J. Plattner, M. R. Alley, S. Cusack, *J. Mol. Biol.* **2009**, *390*, 196. https://doi.org/10.1016/j.jmb.2009.04.073.
[6] R. Gujjar, A. Marwaha, J. White, L. White, S. Creason, D. M. Shackleford, J. Baldwin, W. N. Charman, F. S. Buckner, S. Charman, P. K. Rathod, M. A. Phillips, *J. Med. Chem.* **2009**, *52*, 1864.
[7] T. Umar, S. Gusain, M. K. Raza, S. Shalini, J. Kumar, M. Tiwari, N. Hoda, *Bioorg. Med. Chem.* **2019**, *27*, 3156.
[8] E. Nicolai, G. Cure, J. Goyard, M. Kirchner, J. Teulon, A. Versigny, M. Cazes, F. Caussade, A. Virone-Oddos, A. Cloarec, *J. Med. Chem.* **1994**, *37*, 2371.
[9] P. K. Singh, S. Choudhary, A. Kashyap, H. Verma, S. Kapil, M. Kumar, M. Arora, O. Silakari, *Bioorg. Chem.* **2019**, *88*, 102919.
[10] W. Yu, C. Goddard, E. Clearfield, C. Mills, T. Xiao, H. Guo, J. D. Morrey, N. E. Motter, K. Zhao, T. M. Block, A. Cuconati, X. Xu, *J. Med. Chem.* **2011**, *54*, 5660.
[11] T. A. Farghaly, S. M. Riyadh, M. A. Abdallah, M. A. Ramadan, *Acta Chim. Slov.* **2011**, *58*, 87.
[12] G. Hassan, M. El-Sherbeny, M. El-Ashmawy, S. Bayomi, A. Maarouf, F. Badria, *Arabian J. Chem* **2017**, *10*, S1345. https://doi.org/10.1016/j.arabjc.2013.04.002.
[13] Y. Liu, R. Qu, Q. Chen, J. Yang, N. Cong-Wei, X. Zhen, G. Yang, *J. Agric. Food Chem.* **2016**, *64*, 4845.
[14] V. Pogaku, K. Gangarapu, S. Basavoju, K. K. Tatapudi, S. B. Katragadda, *Bioorg. Chem.* **2019**, *93*, 103307.
[15] J. Wang, M. Sánchez-Roselló, J. L. Aceña, C. del Pozo, A. E. Sorochinsky, S. Fustero, V. A. Soloshonok, H. Liu, *Chem. Rev.* **2014**, *114*, 2432.
[16] S. Zhao, Y. Zhang, H. Zhou, S. Xi, B. Zou, G. Bao, L. Wang, J. Wang, T. Zeng, P. Gong, X. Zhai, *Eur. J. Med. Chem.* **2016**, *120*, 37.
[17] https://www.who.int/news-room/detail/27-04-2020-who-timeline—covid-19
[18] P. Calligari, S. Bobone, G. Ricci, A. Bocedi, *Viruses* **2020**, *12*, 445. https://doi.org/10.3390/v12040445.
[19] O. Aly, *Chem. Rxiv* **2020**. https://doi.org/10.26434/chemrxiv.12061302.v1.
[20] D. Gentile, V. Patamia, A. Scala, M. T. Sciortino, A. Piperno, A. Rescifina, *Mar. Drugs* **2020**, *18*, 225. https://doi.org/10.3390/md18040225.
[21] M. Hoffmann, H. Kleine-Weber, S. Schroeder, N. Krüger, T. Herrler, S. Erichsen, T. S. Schiergens, G. Herrler, H. Wu, A. Nitsche, M. A. Müller, C. Drosten, S. Pöhlmann, *Cell* **2020**, *181*, 271. https://doi.org/10.1016/j.cell.2020.02.052.
[22] H. K. Mahmoud, B. H. Asghar, M. F. Harras, T. A. Farghaly, *Bioorg. Chem.* **2020**, *105*, 104354.

[23] S. A. Al-Hussain, T. A. Farghaly, M. E. A. Zaki, H. G. Abdulwahab, N. T. Al-Qurashi, Z. A. Muhammad, *Bioorg. Chem.* **2020**, *105*, 104330.
[24] M. A. Omar, G. S. Masaret, E. M. H. Abbas, M. M. Abdel-Aziz, M. F. Harras, T. A. Farghaly, *Bioorg. Chem.* **2020**, *104316*, 104.
[25] H. K. Mahmoud, T. A. Farghaly, H. G. Abdulwahab, N. T. Al-Qurashi, M. R. Shaaban, *Eur. J. Med. Chem.* **2020**, *208*, 112752.
[26] T. A. Farghaly, A. M. Abo Alnajab, H. A. El-Ghamry, M. R. Shaaban, *Bioorg. Chem.* **2020**, *102*, 104103.
[27] N. A. Abdel Latif, E. M. H. Abbas, T. A. Farghaly, H. M. Awad, *Russ. J. Org. Chem.* **2020**, *56*(6), 1096.
[28] T. A. Farghaly, G. S. Masaret, Z. A. Muhammad, M. F. Harras, *Bioorg. Chem.* **2020**, *98*, 103761.
[29] R. Shah, T. M. Habeebullah, F. Saad, I. Althagafi, A. Y. Al-dawood, A. M. Al-Solimy, Z. A. Al-Ahmed, F. Al-Zahrani, T. A. Farghaly, N. El-Metwaly, *Appl. Organomet. Chem.* **2020**, *43*, 5886.
[30] H. K. Mahmoud, H. A. Katouah, M. F. Harras, T. A. Farghaly, *Med. Chem.* **2020**, *16*, 761. https://doi.org/10.2174/1573406415666190716153425.
[31] A. F. Kassem, F. Alshehrei, E. M. H. Abbas, T. A. Farghaly, *Mini-Rev. Med. Chem.* **2020**, *20*, 418.
[32] A. M. R. Alsaedi, T. A. Farghaly, M. R. Shaaban, *Molecules* **2019**, *24*, 4009. https://doi.org/10.3390/molecules24214009.
[33] A. S. Shawali, T. A. Farghaly, *Arkivok* **2008**, *I*, 18.
[34] A. S. Shawali, M. A. Abdalla, M. A. N. Mosselhi, T. A. Farghaly, *Heteroatom Chem.* **2002**, *13*(2), 136.
[35] M. A. N. Mosselhi, M. A. Abdalla, T. A. Farghaly, A. S. Shawali, *Monatsch. Chem.* **2004**, *135*, 211.
[36] A. S. Shawali, M. A. N. Mosselhi, T. A. Farghaly, *Phosphorus Sulfur Silicon* **2005**, *180*, 2391.
[37] S. M. Riyadh, T. A. Farghaly, M. A. Abdallah, M. M. Abdalla, M. R. A. El-Aziz, *Eur. J. Med. Chem.* **2010**, *45*, 1042.
[38] S. A. Al-Hussain, F. Alshehrei, M. E. A. Zaki, M. F. Harras, T. A. Farghaly, Z. A. Muhammad, *J. Heterocycl. Chem* **2021**, *58*, 589.
[39] W. E. Truce, E. M. Kreider, W. W. Brand, *Organic Reactions* **1970**, *18*, 99. https://doi.org/10.1002/0471264180.or018.02 ISBN 0471264180.
[40] A. M. Abo Alnaja, T. A. Farghaly, H. S. A. El-zahabi, M. R. Shaaban, *Med. Chem.* **2020**, in press. *17*, 501. https://doi.org/10.2174/1573406416666191216120301.
[41] U. P. Singh, H. R. Bhat, P. Gahtori, R. K. Singh, *In Silico Pharmacol.* **2013**, *1*, 3.
[42] S. Kim, S. W. Lee, E. C. Choi, S. Y. Choi, *Appl. Microbiol. Biotechnol.* **2003**, *61*, 278. https://doi.org/10.1007/s00253-003-1243-5.
[43] U. A. Ochsner, X. Sun, T. Jarvis, I. Critchley, N. Janjic, *Exp. Opin. Invest. Drugs* **2007**, *16*, 573. https://doi.org/10.1517/13543784.16.5.573.
[44] G. H. Vondenhoff, A. Van Aerschot, *Eur. J. Med. Chem.* **2011**, *46*, 5227. https://doi.org/10.1016/j.ejmech.2011.08.049.
[45] P. C. Lv, H. L. Zhu, *Curr. Med. Chem.* **2012**, *19*, 3550. https://doi.org/10.2174/092986712801323199.
[46] P. Sang, S. Tian, Z. Meng, L. Yang, *RSC Adv.* **2020**, *10*, 15775. https://doi.org/10.1039/d0ra01899f.
[47] R. Cruickshank, J. P. Duguid, B. P. Marion, R. H. A. Swain, *Medicinal Microbiology, Vol. II*, 12th ed., Vol. 196, Churchill Livingstone, London, England **1975**.
[48] Molecular Operating Environment (MOE) 2014.09, Chemical Computing Group Inc., 1010 Sherbrooke Street West, Suite 910, Montréal, H3A 2R7, Canada, http://www.chemcomp.com

SUPPORTING INFORMATION

Additional supporting information may be found online in the Supporting Information section at the end of this article.

How to cite this article: Muhammad ZA, Farghaly TA, Althagafi I, Al-Hussain SA, Zaki MEA, Harras MF. Synthesis of antimicrobial azoloazines and molecular docking for inhibiting COVID-19. *J Heterocyclic Chem*. 2021;58: 1286–1301. https://doi.org/10.1002/jhet.4257